

# Texture Evolution during Thermal Processing of Ti-6Al-4V: A Neutron Diffraction Study

Perumal, B., Gungor, S., Kockelmann, W., Fitzpatrick, M. & Bhavani, P.

Published PDF deposited in Coventry University's Repository

**Original citation:**

Perumal, B, Gungor, S, Kockelmann, W, Fitzpatrick, M & Bhavani, P 2021, 'Texture Evolution during Thermal Processing of Ti-6Al-4V: A Neutron Diffraction Study', SVOA Materials Science & Technology, vol. 3, no. 2, pp. 13-23.

<https://sciencevolks.com/materials-science/abstract.php?id=MTMw/>

ESSN 2634-5331

Publisher: ScienceVolks

**This is an open access article distributed under the Creative Commons Attribution License, which permits unrestricted use, distribution, and reproduction in any medium, provided the original work is properly cited.**

# Texture Evolution during Thermal Processing of Ti-6Al-4V: A Neutron Diffraction Study

Bama Perumal\*<sup>1</sup>, Salih Gungor<sup>2</sup>, W. Kockelmann<sup>3</sup>, Michael E. Fitzpatrick<sup>1</sup> and P. Bhavani<sup>4</sup>

## Affiliation:

<sup>1</sup>Faculty of Engineering, Environment and Computing, Coventry University, Coventry CV1 5FB, United Kingdom

<sup>2</sup>Materials Engineering, The Open University, Walton Hall, Milton Keynes, MK7 6AA, United Kingdom

<sup>3</sup>Rutherford Appleton laboratory, ISIS Facility, OX11 0QX, United Kingdom

<sup>4</sup>Assistant Professor, Department of Chemistry, Rajeswari Vedachalam Government Arts College, Chengalpattu -603001, India

\*Corresponding Author: Bama Perumal, Faculty of Engineering, Environment and Computing, Coventry University, Coventry CV1 5FB, United Kingdom

Received: March 24, 2020 Published: April 01, 2021

## Abstract:

This paper reports results of phase transformation experiments in the  $\alpha/\beta$  alloy Ti-6Al-4V from  $\alpha \rightarrow \beta \rightarrow \alpha$  on heating below and near the  $\beta$ -transus using *in situ* neutron diffraction. The development and evolution of crystallographic texture during the  $\alpha \rightarrow \beta \rightarrow \alpha$  phase transformation was determined. Annealing at a sub-transus temperature 1562K (850°C) shows similar  $\alpha$ -phase and  $\beta$ -phase pole figures from room temperature up to 1562K (850°C), with a slight increase in the intensity of the  $\beta$ -phase pole figures, showing that the  $\beta$ -phase texture strengthens during heating. During cooling, the  $\beta \rightarrow \alpha$  transformation occurs very quickly and the initial alpha-texture obtained at room temperature is significantly weakened by the heat-treatment. Strengthening of the  $\beta$ -phase texture is observed on heating the sample from [1163K to 1253K (890°C to 980°C), respectively] and a Burgers relationship ( $(0002) \alpha / (110) \beta$  and  $\{11-20\} \alpha / \{111\} \beta$ ) is seen with the  $\alpha$ -phase texture at room temperature; but no evidence of variant selection was observed during  $\alpha \rightarrow \beta$  transformation. During the  $\beta \rightarrow \alpha$  phase transformation on cooling, the Burgers relationship holds. This indicates a texture memory effect due to the growth of the primary alpha phase present at high temperature.

**Keywords:** Ti-6Al-4V, Neutron Diffraction, Phase Transformation, Texture Evolution, Texture memory effect.

## 1. Introduction

Ti-6Al-4V is a high-performance two-phase ( $\alpha+\beta$ ) titanium alloy used in industrial and medical applications such as turbine blades and knee implants due to its high strength and excellent corrosion resistance. The properties of titanium alloys are strongly dependent on the microstructural and crystallographic texture evolution during thermo-mechanical processing (TMP), which leads to both recrystallization and phase transformation. The crystallographic texture reflects the thermo-mechanical processing history of the material (e.g. plastic deformation, recrystallization, particle rotation and phase transition), and the existence of texture results in anisotropic physical properties. The most commonly used techniques for texture studies in hexagonal zirconium and titanium alloys are EBSD and X-ray diffraction.

In general, the two-phase ( $\alpha+\beta$ ) titanium alloys exhibit moderate-to-strong crystallographic textures that develop during large deformation in the ( $\alpha+\beta$ ) phase field. A low-temperature deformation tends to result in a basal/transverse (B/T) texture while a high-temperature deformation near the beta transus ( $\alpha+\beta \rightarrow \beta$ ) transformation temperature results in a transverse (T) texture [1]. The transformation between the  $\alpha$ -phase and the  $\beta$ -phase of both zirconium and titanium occurs according to the orientation relation  $\{0001\} \langle 1120 \rangle$  (hcp- $\alpha$ )  $\rightarrow$   $\{110\} \langle 111 \rangle$  (bcc- $\beta$ ), observed by Burgers for single crystals [2]. According to this relation, during the  $\alpha \rightarrow \beta$  transition upon heating, six equivalent crystallographic  $\beta$  variants can occur from a single  $\alpha$  orientation. Conversely, during the  $\beta \rightarrow \alpha$  phase transition, there are 12 potential  $\alpha$ -variants. When the material is transformed from the  $\alpha$ -phase to  $\beta$ -phase and back to  $\alpha$ -phase again, the original  $\alpha$ -phase orientations are maintained either perfectly or to some extent: this is called texture memory effect [3]. Jourdan et al. [4] studied a memory effect in single crystals and reported that the crystal returned to the same orientation from which it started during the  $\beta$  to  $\alpha$  transformation.

The selective orientations observed during phase transformation were also investigated in deformed polycrystalline aggregates [5]. For example, zirconium and titanium, which are hot-rolled above their transition temperature and cooled to room temperature (RT), showed a strong rolling texture similar to the starting texture [6, 7]. Under certain conditions individual orientations (or variants) can occur more frequently than others. This phenomenon is known as variant selection. However, in titanium and zirconium alloys there have been reports of variant selections during diffusional phase transformation [8]. For example, in titanium alloys, hot rolling above the  $\beta$  transus and heavy cold rolling near  $\beta$  annealing have both led to transformation with variant selection [9, 10]. In titanium alloy the phase transformations have been linked to either transformation strain or elastic anisotropy [11]. The transformation can occur the influence of external stress or strain. Bhattacharyya et al. [12] observed that in titanium there is a tendency for the prior  $\beta/\beta$  grain boundary to have  $\alpha$  product on either side with close alignment of their (0001) poles. The transformation texture was attributed mainly to variant selection during the hcp $\rightarrow$ bcc $\rightarrow$ hcp phase transformation. Therefore, the texture of the  $\alpha$ -phase has a great influence on the mechanical properties such as the fatigue strength of Ti-6Al-4V. So, the improvement of these properties for a given application requires good control of the induced texture.

In the present study, high-temperature neutron diffraction was undertaken to measure the bcc texture directly at high temperature, and also to determine the texture evolution and variant selections during heating-cooling cycles in both  $\alpha\rightarrow\beta$  and  $\beta\rightarrow\alpha$  transformations in Ti-6Al-4V alloy.

## 2. Materials and experimental procedure

### 2.1 Material

The material used in this investigation was received as a round bar (40 mm diameter and length of about 90 mm) of two-phase  $\alpha + \beta$  titanium alloy Ti-6Al-4V produced by TIMET UK Ltd (Birmingham, UK) and supplied by QinetiQ Ltd (Farnborough, UK). The material was received in the mill-annealed condition, having a measured composition (in wt. %) of 6.48 Al, 3.9 V, 0.15 O, 0.22 Fe, 0.002 N, and 0.02 C, 0.005 H, and balance titanium. The microstructure of the as-received bar was bimodal, i.e., equiaxed alpha in a matrix of the transformed beta. The beta transus temperature was 995° C [13,14].

The as-received equiaxed  $\alpha$  was pre-treated at 1223K (950°C) for 10 minutes and 1303K (1030°C) for 2 minutes (above the beta transus) and water quenched to produce an acicular  $\alpha$  microstructure. These beta-annealed Ti-6Al-4V samples were then heat treated at 1562 K (850°C) and 1796 K (980°C) and water quenched in order to quantify the texture (and microstructure) of the primary alpha present at the soak temperature. In this work, the specimens were evenly coated with a glass lubricant, Acheson Delta glaze FB-412, for protection against high temperature oxidation. Furthermore, on the top of the glass lubricant, a hexagonal-boron nitride lubricant was applied to minimise the specimen-platen interfacial friction. The boron nitride lubricant was utilised to reduce the specimen barrelling and also helps in separating the dies from the specimen after the test. The lower and upper surfaces of the platens were also coated with the same lubricant.

### 2.2 Experimental procedure

Neutron diffraction method is an efficient method to estimate texture information directly from the Rietveld method, which is capable of determining crystal structures based on the whole diffraction spectrum. Quantitative texture measurements utilising X-rays or electrons require careful sample preparation to minimize surface effects and corrections for absorption, but by using neutrons for such measurements all of the above issues are easily avoided. Due to the high penetrating capability of neutrons, bulk texture can be investigated easily. Since the 1960s neutron diffraction has been employed regularly to determine crystallographic textures.

The classical methods are more prone to the problem of overlapping peaks, it is difficult to determine pole figures for minor phases (small volume fractions of beta phase) in multi-phase materials. Because the diffraction peaks of the minor components are much smaller than those of the major components resulting in poor signal-to-background ratio. This is because of the reflected intensity is proportional to the volume fraction of the respective phase. Using, X-ray diffraction there is some limits for texture analysis in order to estimate the minor phase whereas due to the higher penetration depth of neutrons a much larger volume contributes to the reflected intensities in neutron diffraction.

Using time-of-flight (TOF) neutron diffraction, complete spectra with many diffraction peaks, rather than individual peaks, are recorded. Detectors at fixed scattering angles are used to record a whole diffraction spectrum for each sample orientation. The relative intensity changes between the various scattering (hkl) planes present in the different detectors in a bank are indicative of texture. These diffraction peaks confirm that neutron scattering is capable of probing a bulk sample and is well suited for obtaining the texture from a minor  $\beta$ -phase constituent in the Ti-6Al-4V alloy.

The experiments to determine the bulk texture were carried out using the GEM diffractometer instrument at the UK's ISIS neutron source, as shown in Table 1 & 2.

Sample No.	Prior heat treatment	Measured Temperature °C
0	As-received	RT
1	Beta-annealed + Water quenched+30mins@980°C+water quenched	RT
2	Beta-annealed + Water quenched+30mins@850°C+water quenched	RT
3	Beta annealed +Water quenched	RT 780 850 RT
4	Beta annealed +Water quenched	RT 890 920 950 980 950 920 890 280 RT

**Table 1** GEM - temperature cycle test programme

Sample No	Temperature & Strain rate	Measured temperature
5	980°C, 0.1/s, $\epsilon = 1$	RT
6	980°C, 0.1/s, $\epsilon = 1$	RT
7	850°C, 0.1/s, $\epsilon = 1$	RT
8	850°C, 0.1/s, $\epsilon = 1$	RT 780°C 850°C 300°C
9	980°C, 0.1/s, $\epsilon = 1$	RT 980°C RT-300°C RT-120°C

**Table 2:** GEM - Hot deformation test program

GEM (General Materials power diffractometer) is a high-count-rate materials neutron diffractometer (shown in Figure 1) [15]. It is designed to study the structure of both crystalline and amorphous (including liquid) samples [16]. The GEM detector array has 7270 individual detector elements in 86 modules with 6 detector banks (banks 1 and 6 covering forward backscattering angles).

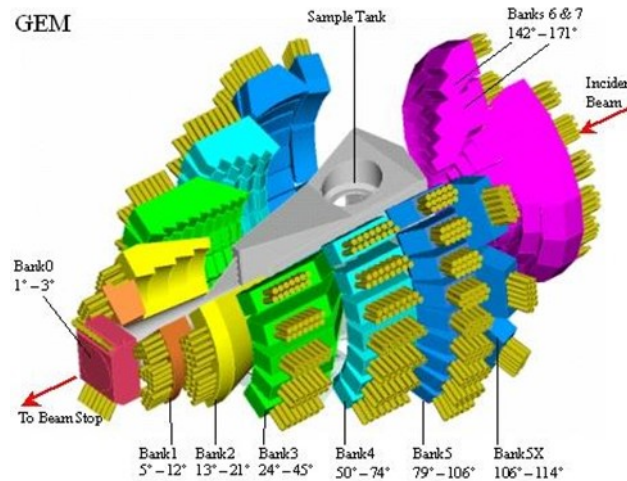


**Figure 1:** A schematic layout of the GEM detector array.

For texture analysis 164 separate detector groups were generated, with each group covering approximately  $10^\circ \times 10^\circ$ . The GEM detectors cover a scattering angle range from  $1.1^\circ$  to  $169.3^\circ$ . The diffraction spectra were measured at different temperatures and each data set for all experimental conditions was collected in 20 minutes. For the heating cycle a sample was mounted in a vanadium holder inside a resistive heating furnace designed for neutron powder diffraction experiments, constructed using vanadium foil heating element and heat shields. The neutron diffraction facility at Rutherford Appleton laboratory provides a wide range of state-of-the-art sample environment equipment to support users with their science programmes. These experiments were carried out using a vacuum furnace, covering the temperature range  $200^\circ\text{C}$  to  $2000^\circ\text{C}$  for the neutron instruments to control environmental issues.

The normal direction of the sample was along the incident beam direction. Data is refined initially for instrument parameters and background, then the crystallographic and microstructural parameters, and finally all parameters including the texture and volume fraction of the phases. For converting relative diffraction intensities to experimental pole figures, it is necessary to carry out data normalisation and corrections for detector efficiencies. The data obtained were normalized to an incident neutron flux distribution and corrected for detector efficiencies using data collected from a solid 8-mm-diameter vanadium rod. The corrected data were converted into 164 d-spacing patterns for the sample orientation corresponding to the detector groups. The diffraction patterns (for all 164) were simultaneously fitted using the Rietveld method in MAUD software [16] for the respective sample orientations. The values of the ODF cells were extracted using the extended WIMV (E-WIMV) algorithm as implemented in MAUD [17]. The E-WIMV method can handle highly irregular as well as incomplete pole figure coverage. No sample-symmetry constraints were imposed on the diffraction analysis. The microstructures that develop during preheating prior to the hot working (Figure 2) were also established for both globular and acicular conditions by heat treatments followed by water quenching. The microstructure evolution of Two-Phase Ti-6Al-4V with different condition was discussed and published [18].

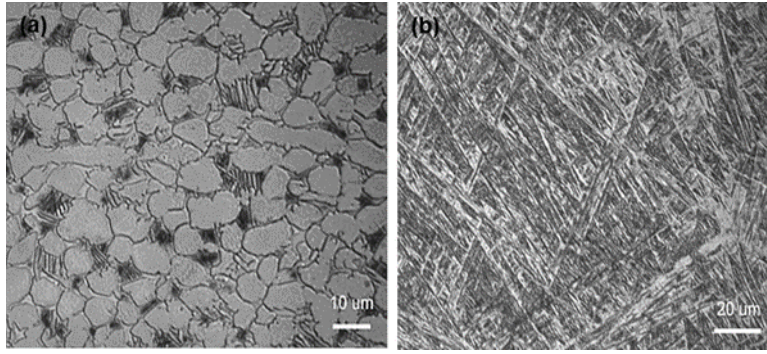


**Figure 2:** Light micrographs showing (a) the as received microstructure, and (b) the same material after heat treatment of 950°C/10min + 1030°C/2min followed by water quenching.

The test specimens were heated at a rate of 1°C per second to the test temperature, then allowed to soak for 30 minutes to get a homogenous distribution of temperature throughout the specimen. The specimens were then deformed under constant true strain rate control to a nominal true strain of 1, in a direction perpendicular to the forging axis of the original bar. The deformed specimens were then water-quenched as quickly as possible, with a typical time delay of 3-12 seconds, in order to preserve the as-deformed texture. In this study, the transverse direction (TD) is parallel to the horizontal axis and RD is parallel to the vertical axis of the cylindrical samples which is perpendicular to the forging axis of the original bar. The three reference axes are labelled as X, Y & Z; known as ND, RD, and TD are shown in Figure 3.

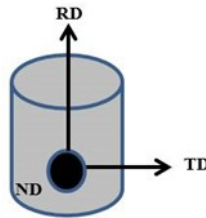


**Figure 3:** A schematic representation of the reference axes.

In the present study, the heating-cooling temperature cycles were carried out at 850° C (sub-transus) and 980° C (near-transus) temperatures in the sequences: 73K (RT) – 1436 K (780° C) – 1562 K (850° C) – 73K (RT); and 73K (RT) – 1634 K (890° C) – 1688 K(920° C) – 1742 K (950° C) – 1796 K (980° C) – 1742 K (950° C) – 1688 K (920° C) – 1634 K (890° C) – 73K (RT). The pole figures show basal (0002), pyramidal (10-10) and prismatic (11-20) textures for the  $\alpha$ -phase and the (100), (110) and (111) texture for the  $\beta$ -phase texture.

### 3. Results and Discussion

#### 3.1 Texture Evolution

##### 3.1.1 As-received texture (Sample No: 0)

The RT (room temperature) texture of globular as-received Ti-6Al-4V was measured with neutron diffraction. The calculated pole figures are shown in Figure 4 (a & b). The  $\alpha$ -phase pole figures of the as-received material at RT show a moderate hcp compression texture with a typical preferred orientation of the {0001} poles to the normal direction (ND).

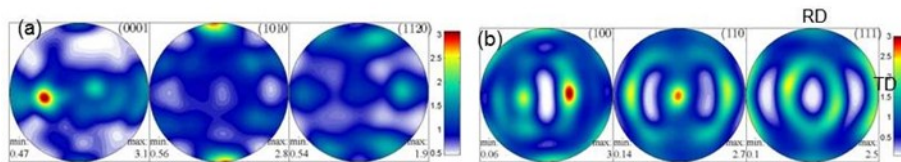


**Figure 4:** As-received (globular) texture of Ti-6Al-4V. (a) Alpha phase texture for the (0002), (10-10) and (11-20) pole figures (b) beta phase texture for the (100), (110) and (111) pole figures calculated at RT.

Luetjering [14] observed a similar texture in two ( $\alpha+\beta$ ) titanium alloys and considered it as a typical rolling texture of Ti-6Al-4V. This initial hexagonal texture shows a broad (0001) maximum in the normal direction. Kocks *et al.* [1] also observed similar texture behaviour on rolled titanium. The (10-10) pole figure shows a maximum in the rolling direction. The (11-20) pole figure also has a maximum in the rolling direction but it is slightly broader than the (10-10) maximum and extended toward the transverse direction.

This typical rolling texture was also found in the starting condition of cold-rolled Zircaloy-2 and Zircaloy-4 sheets [19]. Similar RT texture has also been seen by other researchers for rolled Zircaloy [20] and titanium using neutron diffraction. The obtained beta pole figures as shown in Figure 4(b) for as-received (globular) Ti-6Al-4V showed a maximum around the normal direction (ND) and spread along the transverse direction (TD).

### 3.1.2 Hot-forged texture (Sample no: 5)

The as-received sample was hot-forged at 1796K (980° C) at a strain rate of 0.1/s to a strain of 1, and texture measurements were carried out at RT after water quenching. Hot-forged Ti-6Al-4V at near-transus temperature (Figure 5(a)) shows a similar (0001) pole figure as in the as-received condition (Figure 4(a)) where the (0001) maximum splits more distinctly into two sub maxima.

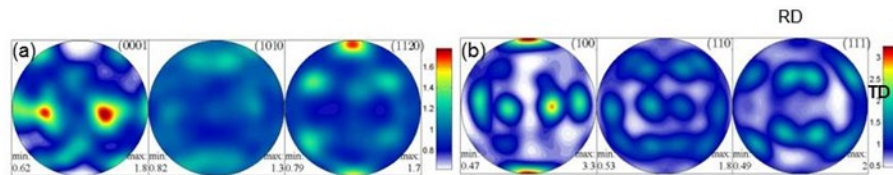


**Figure 5:** Hot forged texture of Ti-6Al-4V at 980°C, 0.1/s and  $\varepsilon = 1$  (a). The alpha phase texture for the (0002), (10-10), (11-20) and (b). The beta phase texture for the (100), (110), (111) pole figures calculated at RT.

The (10-10) maximum for texture near the transus temperature is broadly spread out in the transverse direction compared to the as-received (10-10) pole figure. There is the formation of a new hcp texture observed in the (11-20) pole figure, which has a distinct (11-20) maximum spread out in the rolling direction. This occurs either martensitically or by diffusion-controlled nucleation, with the mechanism depending on cooling rate and alloy composition. The obtained beta phase texture is completely different from the as-received beta-texture. These data clearly indicate, based on observed maximum pole densities, that Ti-6Al-4V hot-forged at 1796K (980° C) at a strain rate of 0.1/s with strain =1 weakens both alpha and beta texture.

### 3.1.3 Beta-annealed texture in the ( $\alpha$ & $\beta$ ) phase (Sample no: 1&6)

At 1796K (980° C), the  $\alpha$ -phase is transformed into the  $\beta$  phase. Figure 6 shows the texture of pre-tested and hot-forged beta-annealed Ti-6Al-4V measured at 1796K (980° C). In Figure 6(a), the pre-test (un-deformed) alpha phase {0001} texture shows sub maxima in the normal direction (ND). The (11-20) pole figure also has a minimum in the RD but is again broader than the (10-10) maximum and extended toward the TD as seen in the as-received globular Ti-6Al-4V at RT (Figure 4 (a)). Figure 6(b) shows similar (100), (110) and (111) pole figures in Figure 6 (a).

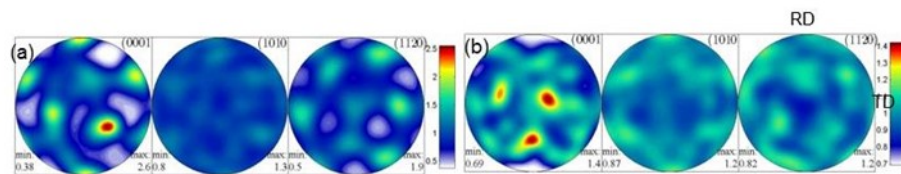


**Figure 6:** The beta-annealed Ti-6Al-4V measured for the (0002), (10-10) and (11-20) pole figures annealed at 980 °C (a). Pre-test (alpha-lamellar) texture annealed at 980°C, (b). Hot-forged texture observed at 980°C, 0.1/s,  $\varepsilon = 1$ .

It is observed from the {10-10} pole figure that the maximum in RD at the {11-20} pole intensity is significantly lower than the pre-test RT measurement and has a large spread towards RD. Figure 7 (a & b) shows the beta-phase texture of pre-tested and hot-forged Ti-6Al-4V measured at 1796K (980° C).

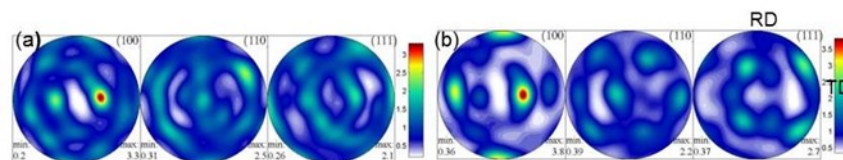


**Figure 7:** Beta-annealed Ti-6Al-4V measured for the (100), (110) and (111) pole figures annealed at 980 °C (a). Pre-test (alpha-lamellar) beta-phase texture (b). Hot-forged beta-phase texture observed at 980°C, 0.1/s,  $\varepsilon = 1$ .

The beta-phase texture observed in Figure 7(a) has similar (100) and slightly different (110) and (111) pole figures, compared to the as-received (globular  $\alpha$ ) measured at 1796K (980° C) (Figure 5(b)), which shows nearly the same intensity. The hot-forged beta-phase texture of Ti-6Al-4V observed at 1796K (980° C), 0.1/s,  $\varepsilon = 1$  (Figure 7 (b)) shows similar (100), (110) and (111) pole figures as compared with Figure 7 (a).

### 3.1.4 Beta-annealed texture in the $\alpha$ phase (Sample no: 2&7)

The neutron-diffraction experiments at RT showed (Figure 4a) that the texture of the  $\alpha$ -phase was sharpened and the intensity of the {0001} preferred orientation along ND was increased as compared to the {0001} pole figure in Figure 5 (a).

In Figure 8(a), {10-10} and {11-20} pole figures are nearly similar in texture as seen in Figure 6(b). The hot-forged (Figure 5(a)) alpha phase texture {0001} looks similar to the alpha phase texture annealed at 1796K (980 °C) (Figure 6 (b)).

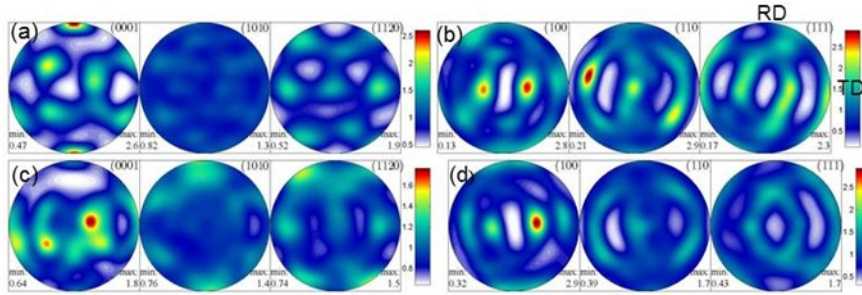


**Figure 8:** The beta-annealed Ti-6Al-4V measured for the (0002), (10-10) and (11-20) of alpha-phase and (100), (110) and (111) of beta-phase annealed at 850 °C (a). Alpha & (b). Beta textures of Pre-tested Ti-6Al-4V annealed at 850°C, (c) Alpha & (d). Beta texture of hot-forged Ti-6Al-4V observed at 850°C, 0.1/s,  $\epsilon = 1$ .

The {10-10} and {11-20} pole densities in the RD are slightly larger than those after initiation of the ( $\alpha \rightarrow \beta$ ) transformation. The beta-phase pole figures of both pre-tested (b) and hot-forged (d) Ti-6Al-4V at 850 °C, 0.1/s,  $\epsilon = 1$  show similar (100) but different (110) and (111) with lower intensity as compared to pre-tested alpha Ti-6Al-4V annealed at 1562 K (850 °C).

### 3.2 Texture evolution during thermal cycling

#### 3.2.1 Analysis of the $\alpha \rightarrow \beta$ texture changes (Sample no: 9)

Gey *et al.* [21-23] observed strong rolling texture in zirconium and titanium when heated above the transition temperature and cooled again: the resulting hcp texture was similar to the starting texture [24-25].

During annealing, there is a significant change in texture which usually develops a component with *c* axes about 30° from the ND and also exhibits axes (11-20) preferentially aligned in the RD. Similar changes during recrystallization have been documented for titanium [19].

In Figure 9 (a) the basal pole figure at RT exhibits a sub maximum near ND but slightly moved towards the transverse direction (TD). The (11-20) pole figure has multiple maxima split 30° from the rolling direction RD, and remains almost constant up to 1562 K (850 °C) but the intensities and positions of the poles start to change.

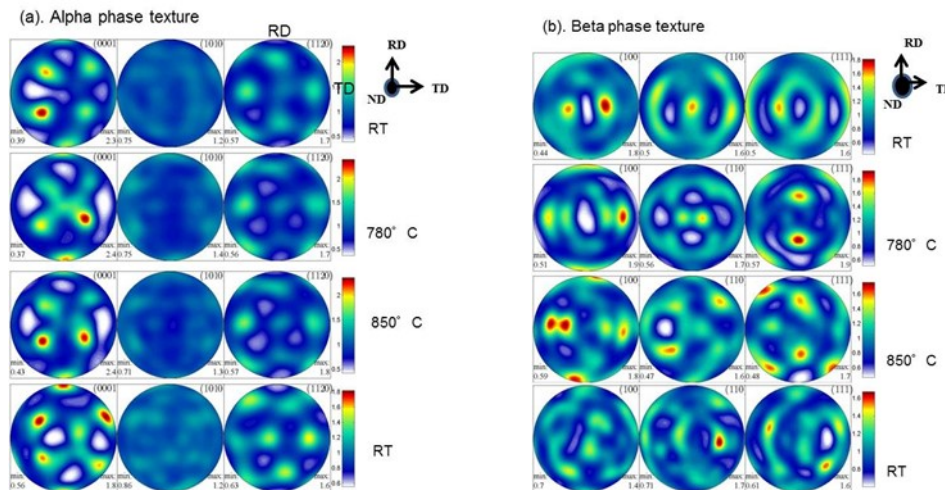


**Figure 9:**  $\alpha$  and  $\beta$  pole figures obtained from in-situ neutron diffraction during a complete  $\alpha \rightarrow \beta$  phase transformation (a) alpha-phase texture during heating to 850 °C (b). Beta-phase texture of Ti-6Al-4V observed during cooling from 850 °C.

Figure 9 (b) illustrates the beta phase texture observed at 1436 K (780 °C) before the start of the  $\alpha \rightarrow \beta$  phase transformation. Two split maxima are observed in the (100) pole figure which is again biased towards the transverse direction, while in the (111) pole figure these have become a strong two maximum parallel to the RD. This type of texture behaviour has been attributed to recrystallization and grain growth and has been reported for both zirconium alloy and commercially pure (CP) titanium [26, 27].

It is noted here that, in the present work, there is no evidence of recrystallization or grain growth during hot compression. During annealing, the alpha to beta transformation starts at 1562 K (850 °C) and finishes at 1823 K (995 °C) (the beta-transus temperature).

Therefore, the transformation at 1562 K (850 °C) is the initial stage of the  $\alpha \rightarrow \beta$  phase transformation. The  $\beta$  pole figures are dominated by a (111) maximum in the RD, while the (110) pole figure exhibits a maximum around ND; the split maxima of the (100) pole figure at 1436 K (780 °C) and 1562 K (850 °C) looks similar with nearly the same intensity. It is also noted that the  $\beta$  pole figures in Figure 9 (b) display a slightly increasing intensity of the dominant texture components, which suggests that the  $\beta$ -phase texture strengthens during heating.

### 3.2.2 Analysis of the $\alpha \rightarrow \beta \rightarrow \alpha$ texture changes (Sample no: 10)

The evolution of  $\alpha$  and the high temperature  $\beta$  texture obtained during a complete  $\alpha \rightarrow \beta \rightarrow \alpha$  phase transformation is given in Figure 10 (a & b), respectively.

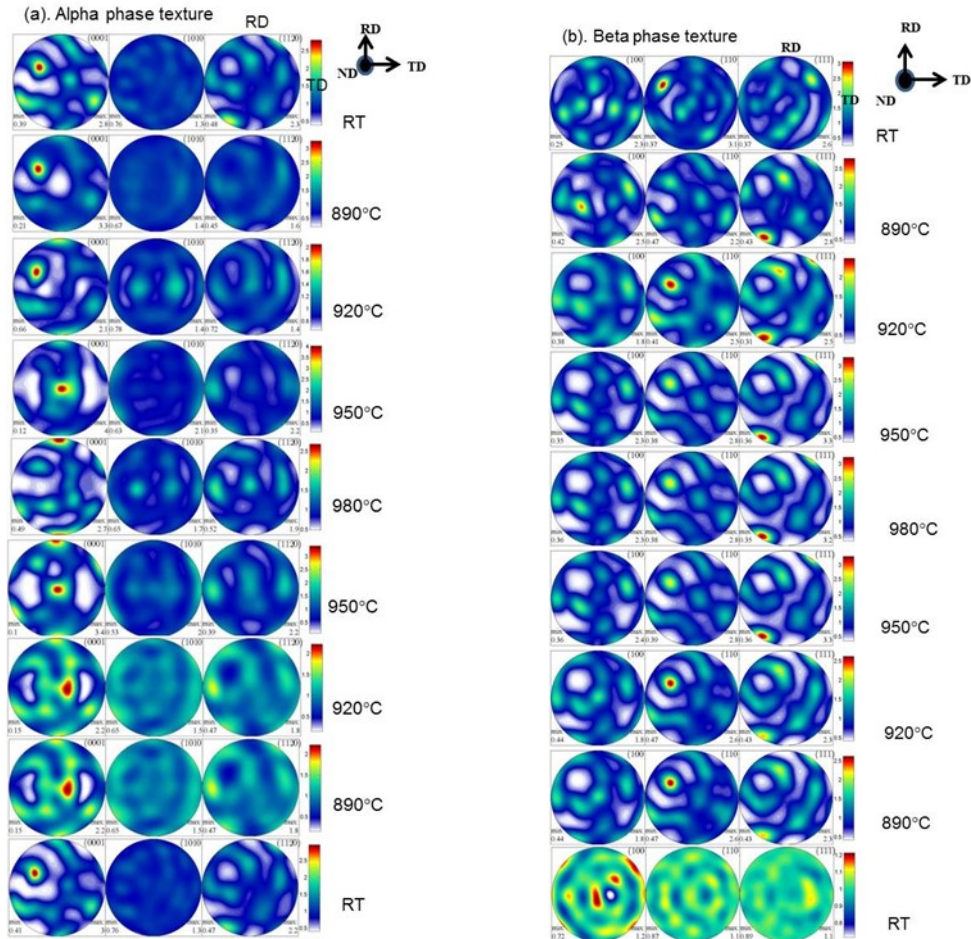


**Figure 10:**  $\alpha$  and  $\beta$  pole figures obtained from in-situ neutron diffraction during a complete  $\alpha \rightarrow \beta \rightarrow \alpha$  phase transformation (a) alpha-phase texture (b). Beta-phase texture.

In this sample,  $\alpha$  and  $\beta$  phases are always present at all conditions, but at different volume fractions. The  $\{10-10\}$  there is a large spread in RD (Figure 10 (a)). At 1634 K (890 °C) the volume fraction of  $\beta$  is estimated at about 40% and the texture of the hexagonal phase is nearly identical to the texture at 1688K (920 °C), where the phase volume fraction of  $\alpha$  is 48% and  $\beta$  is increased to 52%. At 980 °C, the alpha to beta transformation is almost complete; nearly 80% of alpha was transformed to beta. In Figure 10 (a), the initial alpha texture developed at RT is similar to the alpha texture measured at the end of the heat treatment (*i.e.* at RT after cooling from the beta phase). This is the evidence for the texture memory effect during  $\alpha \rightarrow \beta \rightarrow \alpha$  phase transformation. The initial beta texture observed at RT is significantly weakened by the heat-treatment. It slowly drops near the transus temperature and then drops considerably through the complete  $\alpha \rightarrow \beta$  phase transformation. The amount of beta-phase at RT is less than 6%, which is too low for a reliable measurement to estimate its texture.

As seen from Figure 9 (b), the  $\beta$ -phase textures at 1436 K (780 °C) and 1562 K (850 °C) show similar pole figure maxima in terms of their positions in (100), (110) and (111) pole figures. But the beta textures observed at 1634K (890 °C) and 1796K (980 °C) (Figure 10 (b)), during  $\alpha \rightarrow \beta \rightarrow \alpha$  phase transformation show many similarities. It is also noted that the RT beta-texture is different from the high temperature  $\beta$ -phase texture at 1796K (980 °C) as there is an increase in intensity due to the high volume fraction of beta at 1796K (980 °C).

It is evident from Figure 10 (a & b) that during the  $\alpha \rightarrow \beta \rightarrow \alpha$  transformation a preferential variant selection occurred in beta-phase texture and the parallel planes  $\{0002\}_\alpha / \{110\}_\beta$  and  $\{11-20\}_\alpha / \{111\}_\beta$  obtained during measurements confirm that the Burgers orientation relationship is followed.

In previous studies, a strengthening of the  $\beta$  texture was observed in CP titanium [11], which was associated with competitive growth between  $\beta$  grains. SEM and EBSD studies on rolled sheets of CP titanium [26] have shown that, in the early stages of the transformation, there is the possibility of nucleation of  $\beta$ -phase on the grain boundaries and within the grains as plates. Thus, the presence of grain boundary  $\beta$  tends to follow the Burger's relationship with one of the parent grains, whereas intergranular  $\beta$  orientation appears more random. The final stage of  $\alpha \rightarrow \beta \rightarrow \alpha$  phase transformation is a competitive growth of these two types of nuclei and is dominated more by the formation of grain boundary  $\beta$  due to faster moving interfaces. In the present work, if it is assumed that the transformation is likely to occur in a similar manner in Ti-6Al-4V: this can explain the strengthening of the  $\beta$  texture during the phase transformation on heating. Once the sample was cooled down,  $\alpha$  texture was again measured at RT (as shown in Figure 9 (b)). In Figure 10 (a), the  $\{1120\}$  pole in the RT  $\alpha$ -phase is nearly parallel to the direction of the  $\{111\}$  poles of the strong  $\beta$ -phase texture observed at 980 °C at the ND (in figure 10 (b)). In addition to this, the strong  $\{0001\}$  poles of RT  $\alpha$ -phase almost match with the  $\{110\}$  pole in the beta phase at 1796K (980 °C). This is an indication that the Burgers relationship is obeyed for the retransformation from  $\beta$  to  $\alpha$  when the specimen is cooled from the near-transus temperature. In theory, this particular behaviour is expected if the growth of  $\alpha$  forms by nucleation and growth from the  $\beta$  matrix.

### 3.2.3 Analysis of the $\alpha \rightarrow \beta \rightarrow \alpha$ texture changes on - Hot-forged Ti-6Al-4V (Sample No: 8&9)

A complete  $\alpha \rightarrow \beta \rightarrow \alpha$  phase transformation was carried out for the Ti-6Al-4V samples hot-forged at 1562K (850°C) and 1796K (980°C) with a strain rate of 0.1/s and  $\epsilon = 1$ .

After hot-compression at sub-transus and near-transus temperatures, the hot-forged Ti-6Al-4V samples were heated up to the target temperature and cooled again. Figure 11 illustrates the texture evolution of Ti-6Al-4V hot-forged at 1562K (850 °C) with a strain rate of 0.1/s and  $\epsilon = 1$ . This shows very similar alpha phase texture during the complete  $\alpha \rightarrow \beta \rightarrow \alpha$  phase transformation but the  $\beta$ -phase deformed texture shows completely different during  $\alpha \rightarrow \beta \rightarrow \alpha$  phase transformation. The textures of the Ti-6Al-4V sample hot-forged at 1796K (980°C), 0.1/s, and  $\epsilon = 1$  at the start and at the end of the heating cycle are different as shown in Figure 12 (a). In Figure 10, the initial alpha texture developed at RT is similar to the alpha texture measured at the end of the heat treatment (i.e. at RT after cooling).

This is evidence for the texture memory effect of hot-forged Ti-6Al-4V during heating-cooling cycle. The investigation of the  $\beta$ -phase texture of hot-forged Ti-6Al-4V specimens during thermal-cycling led to two different observations. Firstly, the  $\beta$ -phase texture at 1562K (850°C) and 1796K (980°C) (Figures 11 & 12) clearly shows that there are no similarities and not much strengthening of the  $\beta$ -phase texture on heating the sample from 1634K (890°C) to 1796K (980°C).

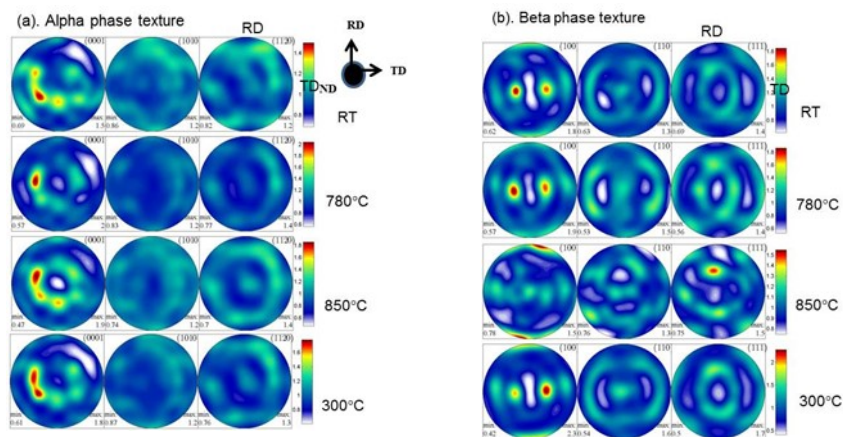


**Figure 11(a & b):**  $\alpha$  and  $\beta$  pole figures obtained during thermal cycle of hot-forged Ti-6Al-4V at 850 °C, 0.1/s, and  $\epsilon = 1$ .

During the heating-cooling cycle, the  $\beta$ -phase textures of heat-treated Ti-6Al-4V specimens show similar  $\beta$ -phase texture at 1634K (890°C) and 1796K (980°C) (as shown in Figure 10 (b)) and there is strengthening of the  $\beta$ -phase texture observed on heating the sample from 1634K (890°C) to 1796K (980°C). Secondly, it is evident from figure 11 that the  $\beta$ -phase texture at 1562K (850°C) does not exhibit the Burgers relationship with the  $\alpha$ -phase texture observed at 1562K (850°C). Furthermore, the comparison between  $\{0002\}_\alpha / \{110\}_\beta$  and  $\{1120\}_\alpha / \{111\}_\beta$  pole figures at 850°C ( $\alpha$ -phase) in Figure 10 and at 1796K (980°C) ( $\beta$ -phase) in Figure 12 show that the pole intensities are similar and thus the Burgers relationship was followed in hot-forged Ti-6Al-4V during transformation from  $\alpha \rightarrow \beta$ . Bhattacharyya *et al.* [28] observed similar behaviour while studying the  $\alpha$  to  $\beta$  phase transformation in hot-forged Ti-6Al-4V using neutron diffraction and concluded that beta phase grew from pre-existing  $\beta$  grains, not by fresh nucleation from the alpha phase.

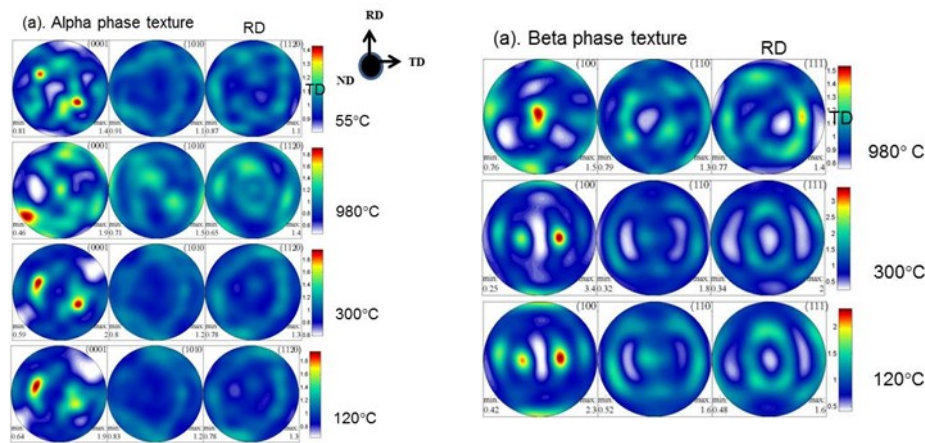


**Figure 12(a & b):**  $\alpha$  and  $\beta$  pole figures obtained during thermal cycle of hot-forged Ti-6Al-4V at 980 °C, 0.1/s, and  $\varepsilon = 1$ .

These results confirm that there is an absence of recrystallization and formation of new grains during hot-forging of Ti-6Al-4V in the ( $\alpha + \beta$ ) phase field (below the beta-transus temperature). It is also evident from Figure 12 that, once the transformation is nearly complete at 1796K (980 °C) (near to transus), the  $\beta$  texture became weak. This is similar to the work of Wenk *et al.* [29] who studied bulk texture evolution in Zircaloy-4 using neutron diffraction. In the present study, no evidence of preferential transformation was found during the  $\alpha \rightarrow \beta$  transformation of hot forged Ti-6Al-4V at 1796K (980 °C), 0.1/s, and  $\varepsilon = 1$ .

#### 4. Conclusions

1. The texture evolution of hcp and bcc hot-forged titanium has been studied *in situ* during thermal cycling using time-of-flight neutron diffraction. The texture analysis indicates definite deviation from the Burgers orientation relationship during hot-compression. It is also noted that during transformation from  $\alpha \rightarrow \beta$ , the pole intensities are similar and thus the Burgers relationship was followed in hot-forged Ti-6Al-4V.
2. The development and evolution of crystallographic texture during the  $\alpha \rightarrow \beta \rightarrow \alpha$  phase transformation was also determined. Annealing at a sub-transus temperature 1562K (850°C) shows similar  $\alpha$ -phase and  $\beta$ -phase pole figures from RT up to 1562K (850°C) but a slight increase in the intensity of the  $\beta$ -phase pole figures was observed. This showed that the  $\beta$ -phase texture strengthens during heating. During cooling, the beta to alpha transformation occurs very quickly and the initial alpha-texture obtained at RT is significantly weakened by the heat-treatment.
3. The RT  $\beta$ -phase texture is completely different from the high temperature  $\beta$ -phase texture at 1796K (980°C). When comparing these two textures, significant differences were observed in terms of texture intensities.
4. The texture observed after hot-compression at 1562K (850°C) with a strain rate of 0.1/s and  $\varepsilon = 1$  shows similar  $\alpha$ -phase texture during the  $\alpha \rightarrow \beta \rightarrow \alpha$  phase transformation but the evolved  $\beta$ -phase textures are dissimilar. Furthermore, no similarity was observed with the sample that was hot-compressed at 1796K (980 °C) for the same strain and strain rate.
5. The strengthening of the  $\beta$ -phase texture is observed on heating the sample from 1634K (890°C) to 1796K (980°C) and these two temperatures show a Burgers relationship ( $(0002)_\alpha / (110)_\beta$  and  $\{11-20\}_\alpha / \{111\}_\beta$ ) with the  $\alpha$ -phase texture at RT. This clearly indicates the presence of a Burgers relationship from  $\alpha \rightarrow \beta$  phase transformation, but no evidence of variant selection was observed during  $\alpha \rightarrow \beta$  transformation. During the  $\beta \rightarrow \alpha$  phase transformation on cooling, the Burgers relationship holds. This indicates a texture memory effect due to the growth of the primary alpha phase present at high temperature. It also appears that there may be a preferential variant selection during  $\beta \rightarrow \alpha$  transformation on cooling.

#### Conflict of Interest

"The authors declare no conflict of interest."

#### Acknowledgements

We gratefully acknowledge the financial support of QinetiQ. The neutron diffraction experiments were performed at the UK ISIS neutron source, and we are grateful to the Science and Technology Facilities Council for awarding beam time. M. E. Fitzpatrick is grateful for funding from the Lloyd's Register Foundation, a charitable foundation helping to protect life and property by supporting engineering-related education, public engagement and the application of research.

## References

1. Kocks, U.F., Tome, C. N. & Wenk, H.-R., Texture and Anisotropy. Cambridge University Press, 1998.
2. Burgers, W.G., Physica, (1934). 1: p. 561
3. Zhu, Z., Liu RY, G.J., Chen, N.P., and Yan, M.G., Mater. Sci. Eng. A, 2000, p. 280.
4. Jourdan, C., Gastaldi, J., Marzo, P., and Grange, G., In situ statistical study of the nucleation, the variant selection and the orientation memory effect during the  $\alpha = \beta$  titanium martensitic transformation. Journal of Materials Science, 1991. 26(16): p. 4355-4360.
5. Gey N. and M. Humbert., Characterization of the variant selection occurring during the  $\alpha + \beta$  phase transformations of a cold rolled titanium sheet. Acta Materialia, 2002. 50(2): p. 277-287.
6. Gey, N., M. Humbert., and H. Moustahfid. Study of the  $\alpha - \beta$  phase transformation of a Ti-6Al-4V sheet by means of texture change. Scripta Materialia, 2000. 42(6): p. 525-530.
7. Wenk, H.R., Lonardelli, I., and Williams, D., Texture changes in the hcp  $\rightarrow$  bcc  $\rightarrow$  hcp transformation of zirconium studied in situ by neutron diffraction. Acta Materialia, 2004. 52(7): p. 1899-1907.
8. Stanford, N., and P.S. Bate., Crystallographic variant selection in Ti-6Al-4V. Acta Materialia, 2004. 52(17): p. 5215-5224.
9. Zhu Zs., G.J., Liu RY, Chen NP, and Yan MG., Mater. Sci. Eng. A, 2000: p.280:199.
10. Gey, N. and M. Humbert, Characterisation of the variant selection occurring during the  $\alpha + \beta$  phase transformations of a cold rolled titanium sheet. Acta Materialia, 2002.50(2): p.277-287.
11. G.C. Obasi, R.J. Moat, D.G. Leo Prakash, W. Kockelmann, J. Quinta da Fonseca, M. Preuss., In situ neutron diffraction study of texture evolution and variant selection during  $\alpha \rightarrow \beta \rightarrow \alpha$  phase transformation in Ti-6Al-4V. Acta Materialia 2012 December; 60(20): 7169-7182.
12. Bhattacharyya, D., Viswanathan, G.B., Denkenberger R., Furrer D and Fraser, Hamish L., Acta Materialia, 2003.51: p.4679.
13. Semiatin, S.L., and Bieler T., Effect of texture and slip mode on the anisotropy of plastic flow and flow softening during hot working of Ti-6Al-4V. Metallurgical and Materials Transactions A, 2001. 32(7): p. 1787-1799.14.
14. Luetjering, G., Influence of processing on microstructures and mechanical properties of  $\alpha + \beta$  titanium alloys. Mater. Sci. Eng., 1998. A243: p.32-45
15. Day, P., Enderby, J.E., Williams, W.G., Chapon, L.C., Hannon, A.C., Radaelli, P.G., and Soper, A.K., Neutron News 15. (2004) p. 19.
16. Lutterotti L., M.S., and Wenk H-R., 12th International Conference Texture of Materials (ICOTOM-12). (Montreal, 9-13 August 1999) ed J.A Szpuna (Montreal: NRC Research press) 1999: p. 1599-604.
17. H.-R. Wenk, H-R., Lutterotti, L., Vogel, S., Texture analysis with the new HIPPO TOF diffractometer. Nuclear Instruments and Methods in Physics Research A 515 (2003) 575-588.14.
18. Bama Perumal, Salih Gungor, J.W. Brooks and Michael E. Fitzpatrick. The Effect of Hot Deformation Parameters on Microstructure Evolution of the  $\alpha$ -Phase in Ti-6Al-4V, Metallurgical and Materials Transactions A 47(8) May 13, 2016 4128—VOLUME 47A, AUGUST 2016.
19. Wagner, F., Bozzolo, N., Van Landuyt, O., and Grosdidier, T., Evolution of recrystallisation texture and microstructure in low alloyed titanium sheets. Acta Materialia, 2002. 50(5): p. 1245-1259.
20. Ciurchea, D., Pop, A. V., Gheorghiu, C., FurtunÇŽ, I., TodicÇŽ, M., Dinu, A., and M. Roth, Texture, morphology and deformation mechanisms in  $\hat{I}^2$ -transformed Zircaloy-4. Journal of Nuclear Materials, 1996. 231(1-2): p. 83-91.
21. Gey, N. and M. Humbert, Characterization of the variant selection occurring during the  $\alpha + \beta$  phase transformations of a cold rolled titanium sheet. Acta Materialia, 2002. 50(2): p. 277-287.
22. Gey, N., M. Humbert, and H. Moustahfid, Study of the  $\alpha - \beta$  phase transformation of a Ti-6Al-4V sheet by means of texture change. Scripta Materialia, 2000. 42(6): p. 525-530.

23. Lonardelli L, Gey N., Wenk HR., Humbert M., Vogel S., and Lutterotti L., *Acta Materialia*, 2007. 55: p. 5718.
24. M.R. Daymond, R.A. Holt, S. Cai, P. Mosbrucker, S.C. Vogel., Texture inheritance and variant selection through an hcp–bcc–hcp phase transformation, *Acta Materialia* 58 (2010), p. 4053–4066.
25. G.A. SARGENT, K.T. KINSEL, A.L. PILCHAK, A.A. SALEM, and S.L. SEMIATIN, Variant Selection During Cooling after Beta Annealing of Ti-6Al-4V Ingot Material, *Metallurgical and Materials Transactions A* October 2012, 43(10), DOI: 10.1007/s11661-012-1245-y
26. A. L. Pilchak, G. A. Sargent, and S. Lee Semiatin., Early Stages of Microstructure and Texture Evolution during Beta Annealing of Ti-6Al-4V, *Metallurgical and Materials Transactions A* 49(9), December 2017, DOI: 10.1007/s11661-017-4444-8.
27. Whittaker, M.T., Evans, W. J., Lancaster, R., Harrison, W., and Webster, P. S., The effect of microstructure and texture on mechanical properties of Ti6-4. *International Journal of Fatigue*, 2009. 31(11-12): p. 2022-2030.
28. Bhattacharyya, D., Viswanathan, G. B., Vogel, S. C., Williams, D. J., Venkatesh, V., and Fraser, H. L., A study of the mechanism of  $\alpha \rightarrow \beta$  phase transformation by tracking texture evolution with temperature in Ti-6Al-4V using neutron diffraction. *Scripta Materialia*, 2006. 54(2): p. 231-236
29. Wenk HR., Lonardelli I., and Williams D., *Acta Materialia*, 2004. 52: p. 1899.

**Citation:** Bama Perumal, Salih Gungor, W. Kockelmann, Michael E. Fitzpatrick and P. Bhavani. "Texture Evolution during Thermal Processing of Ti-6Al-4V: A Neutron Diffraction Study". *SVOA Materials Science & Technology*, 2021, 3(2) Pages: 13-23.

**Copyright:** © 2021 All rights reserved by Bama Perumal et al. This is an open access article distributed under the Creative Commons Attribution License, which permits unrestricted use, distribution, and reproduction in any medium, provided the original work is properly cited.